PHYSICAL REVIEW B **72**, 014109 (2005)

Electronic and structural properties of SnO under pressure

N. E. Christensen and A. Svane
Department of Physics and Astronomy, University of Aarhus, DK-8000, Aarhus C, Denmark

E. L. Peltzer y Blancá
Grupo de Estudio de Materiales y Dispositivos Electrónicos (GEMyDE), Facultad de Ingeniería, UNLP, IFLYSIB-CONICET, C.C. No. 565, 1900 La Plata, Argentina

(Received 15 March 2005; revised manuscript received 10 May 2005; published 8 July 2005)

Pressure-induced changes in the electronic and structural properties of tin monoxide are examined by means of *ab initio* density-functional calculations. Also, the pressure shifts of the A_{1g} and E_g zone-center phonon modes are derived. The results are compared to recent experimental high-pressure data as well as to previous calculations for ambient conditions. In agreement with earlier findings we observe that the Sn-5*s* lone pair is not inert but hybridizes with the O-*p* states. Differences in that respect between SnO and PbO are shown to be a "relativistic dehybridization effect" caused by the large mass-velocity downshift of the Pb-6*s* states. SnO is a small-gap (indirect) semiconductor at ambient pressure, but an insulator-metal transition occurs as pressure is applied. The transition is estimated to occur around 5 GPa. The gap depends sensitively on the distance between the layers $dE_{\mathrm{gap}}/d\ln(c/a) \approx 21$ eV.

DOI: 10.1103/PhysRevB.72.014109 PACS number(s): 71.20.Ps, 61.50.Lt, 63.20.Dj

I. INTRODUCTION

Tin oxides SnO and SnO_2 are of considerable technological interest. They, mainly the dioxide, are applied in thin heat reflecting foils, transparent electrodes, gas sensors and Sn-oxide/Si solar cells. Applications of SnO have been less frequent, mainly due to its tendency to decompose (into Sn and SnO_2) at elevated temperatures. Consequently, the monoxide was in the past not examined as much in detail as SnO_2. But during the latest few years several experimental and theoretical studies, also of SnO, were published, mainly to analyze the difference in bonding in the two tin oxides. Under ambient conditions they crystallize in the tetragonal litharge (SnO) and rutile (SnO_2) structures,[1] see Fig. 1.

Transformations under pressure to orthorhombic structures have been reported,[2–4] but the most recent experiments by Wang *et al.*[5] on SnO up to 20 GPa showed no indication of transformation to a lower symmetry than that of the ambient-pressure structure. A broadening was observed[5] of the diffraction lines near 14 GPa, but the structural changes reported earlier were observed at much lower pressures ≈6 GPa, and in Ref. 5 it is suggested that this could be caused by a nonhydrostatic pressure component due to the pressure transmitting medium.

The electronic structure of SnO has not been examined in great detail by experimental methods. It is generally assumed that the monoxide is a semimetal or a small-gap semiconductor. An optical gap of ≈2.5 eV was quoted in Ref. 6, whereas the *fundamental* gap has been mentioned[7] to be 0.7 eV. *Ab initio* calculations[8] showed that the minimum gap is indirect (Γ to M in the Brillouin zone) (in contrast to SnO_2 where the fundamental gap is direct), and this was also found in later theoretical calculations.[9,10] These three investigations included determination of the structural parameters, axial ratios and atomic coordinates, at zero pressure, and found, as in the pseudopotential study by Meyer *et al.*,[11] good agreement with experiments. An important part of the theoretical work by Raulot *et al.*[10] concerns the discussion of the role of the Sn 5*s lone pair* in the bonding of SnO as well as a dicussion of similarities and differences between this case and that of the Pb-6*s* states in α-PbO (also the layered litharge structure). As concluded earlier by Trinquier and Hoffmann[12] and by Terpstra *et al.*[13] the lone pair was shown to play an essential role in the bonding, and it is thus not

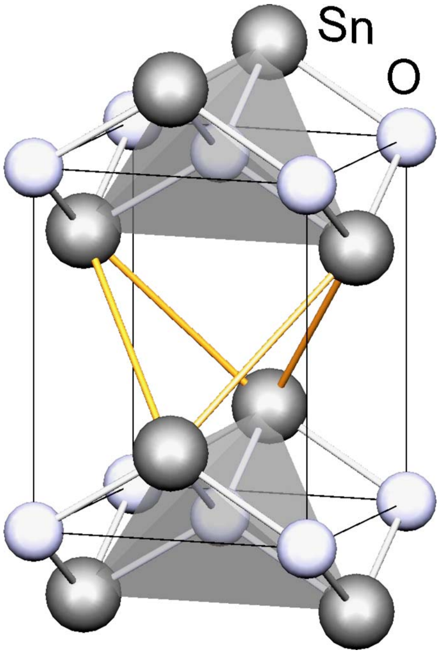

FIG. 1. (Color online) The SnO litharge-type tetragonal structure. The space group is $P4/nmm$ (No. 129). Sn (large spheres) occupy the Wyckoff 2c sites $(0.5,0,u)$ and $(0,0.5,1-u)$, whereas the oxygen atoms are at 2*a* sites (0,0,0) and (0,0.5,0). (From Ref. 5).

1098-0121/2005/72(1)/014109(9)/$23.00

inert, as was also pointed out in Ref. 9. Watson *et al.*[14] showed that the "classical" hybridization theory where the cation-*s* states interacts with *p* states also on the cation is wrong in these compounds, where the lone pairs hybridize with the O-*p* states. The detailed analysis by Raulot *et al.* confirms this and that the intraslab interactions dominate. On the other hand, the indirect fundamental gap depends sensitively on the distance between layers.

The present paper describes some of the aspects mentioned above, but our *ab initio* calculations further include the effects of applying external pressure. This allows us to compare to recent high-pressure experiments,[5] including the structural changes in axial ratio (c/a) and u, see caption to Fig. 1, as well as Γ-phonon frequencies. The density-functional calculations are carried out whithin the local density approximation (LDA) as well as by application of a generalized gradient approximation (GGA). Section II briefly describes the methods which we use, and results for structure, phonon frequencies, and electric field gradients (EFGs) are given in Sec. III. Band structures, estimate of the insulator-metal transition pressure, and hybridization effects are discussed in Sec. IV, where we also make a few comparisons between SnO and PbO, mainly discussing relativistic effects. The last Sec. V, contains summary and conclusions.

II. METHODS OF CALCULATION

The present density-functional calculations are performed within two approximations, the LDA (Ref. 15) and a GGA. We used the LDA version for exchange and correlation as given by Ceperley and Alder[16] and parametrized by Perdew and Zunger.[17] For the GGA we chose the Perdew-Burke-Ernzerhof (PBE) version.[18] The LDA leads to overbinding, i.e., too small equilibrium volumes, whereas GGA often leads to better values for such basic ground-state quantities. However, it is not unusual that some GGA implementations in fact "overcorrect" for the LDA error in volume, and the present case, SnO, is one where this happens. The PBE formalism improves over the previous Perdew-Wang (PW91) version[19] in an accurate description of the linear response of the uniform gas, behaving correctly under uniform scaling and giving a smoother potential. The PBE-GGA retains the correct features of L(S)DA ("S" for spinpolarized) and combines them with the most energetically important features of gradient corrected nonlocality. Studies of atomization energies for small molecules[18] gave essentially the same results as PW91. However, a remaining uncertainty relates to the value of the parameter κ which is associated to the degree of localization of the exchange-correlation hole. In their original work PBE proposed to use $\kappa=0.804$, but it has appeared[20–23] that, depending on the type of bonding, applications to solids are improved if other values are used. In the present work we found that $\kappa=0.804$ leads to a significant overestimation of the equilibrium volume of SnO, and therefore we used a reduced value, $\kappa=0.60$. In fact, even this is somewhat too large, it appears, but an optimal parameter fit is not the purpose of this work. Pressures (P) vs volume (V) were obtained by analytical differentiation of a power series in $X=(V_0/V)^{1/3}$ least-squares fitted to the total energies calculated for fully optimized structures at 15 or 16 volumes in the range considered (0.80–$1.10V_0$ in the present work, where V_0 is an experimental equilibrium volume). The method requires an accurate fit, r.m.s. errors less than typically 0.01 mRy/f.u. for the energies. The method has been applied to many different systems, see, for example, Refs. 24–26, and references therein.

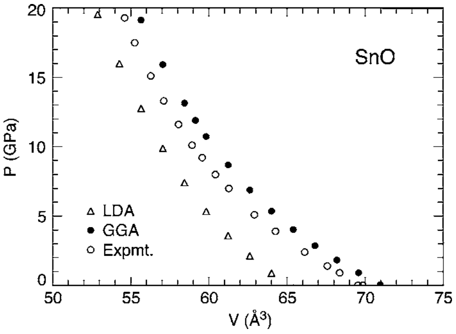

FIG. 2. Pressure P versus volume V for SnO. Experimental results, open circles, are from Ref. 5, whereas the triangles are calulated within the LDA and filled circles give the GGA results. There are two experimental zero-pressure volumes marked, one obtained before pressure was applied and one after, see Ref. 5. In the text and other captions we use an "experimental" reference volume V_0. This was chosen to be 69.578 Å^3.

The linear-muffin-tin-orbital (LMTO) method[27] was used to solve the formal one-particle Kohn-Sham equations. A full-potential (FP) (no spherical averaging of the potentials) LMTO version was used in order to allow accurate structural optimizations. The version is based on the code developed by Methfessel,[28,29] modified by van Schilfgaarde,[30] Novikov,[31] and others. It allows for a simultaneous optimization of lattice axial ratios, angles, and atomic coordinates. A so-called "triple-κ" basis set was used (κ refers here to the decay constant of the MTOs outside the muffin-tin spheres). For Sn, angular momenta up to $\ell=(3,2,2)$ were included in the three channels, whereas a (2,2,2)-basis set was used on oxygen. The semicore Sn-4d states were included as local orbitals.[32] Empty muffin-tin spheres were included for accuracy of interpolation of the nonspherical charge density. Usually no orbitals were associated with these, but tests of basis set convergence, in particular in connection with the phonon calculations, were made with s and p orbitals on the E sites.

The phonon calculations were performed by means of the FP-LMTO method as well as the full-potential linear augmented plane wave (FP-LAPW) method using the WIEN2K code.[33] For illustration of hybridization and calculations of

TABLE I. Calculated equilibrium volumes V_0^{th} and bulk moduli $B_0(V_0^{\mathrm{th}})$ and $B_0(V_0^{\mathrm{exp}})$ (in GPa) evaluated at the theoretical and experimental equilibrium volumes, respectively. $V_0^{\mathrm{exp}}=V_0=69.578$ Å^3. Experimental values for the bulk modulus are. 38 GPa (Ref. 5 and 48±5 GPa (Ref. 3. See also Ref. 28 in Ref. 8.

	$V_0^{\mathrm{th}}/V_0^{\mathrm{exp}}$	$B_0(V_0^{\mathrm{th}})$	$B_0(V_0^{\mathrm{exp}})$
LDA	0.936	47.6	38.4
GGA	1.021	41.0	44.1

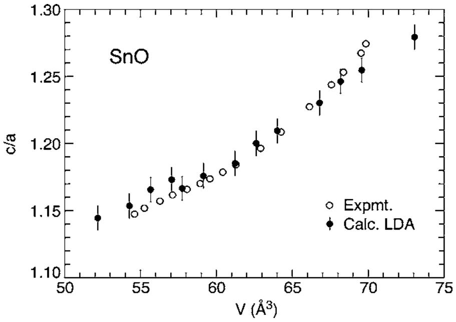

FIG. 3. Axial ratio as calculated (filled circles) within the local density approximation and experimental results Ref. 5. Error bars on the theoretical points correspond to an energy tolerance of 50 μRy/f.u. in the optimization process.

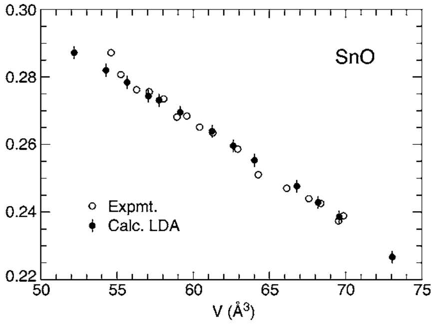

FIG. 5. Parameter u as calculated (filled circles) within the local density approximation and experimental results Ref. 5. Error bars on the theoretical points correspond to an energy tolerance of 50 μRy in the optimization process.

electron localization functions[34,35] (ELFs) we used the tight-binding LMTO method in the atomic-spheres approximation (TB-LMTO-ASA) as implemented in the STUTTGART code, Ref. 36.

Integrations in k space were performed by means of the tetrahedron method,[37–39] using a minimum of 550 points in the irreducible Brillouin zone (IBZ). However, realizing that the LDA/GGA underestimates the minimum gap of SnO, we performed in several cases, for example, for the calculations of phonon frequencies and the EFGs, additional calculations applying a direct sampling over full bands so that the small electron pocket in the conduction band near the M point is not included ("semiconductor" integration mode). This avoids errors due to unphysical metal-insulator transitions when the atomic positions are varied. Further, higher densities, more than 2200 points in the IBZ, were used.

III. RESULTS

This section summarizes the results obtained for structural parameters $c/a, u$, pressure-volume relations, phonon frequencies, and electric field gradients.[40,41]

From the calculated total energies for a series of volumes we derived the pressure-volume relations, see Fig. 2. As mentioned earlier, the LDA leads to overbinding, in this case by $\approx 6\%$, whereas the GGA, here even with reduced κ (0.60), gives a too large equilibrium volume. Further, the present calculations do not include contributions from the lattice vibrations which, even at zero temperature, would increase the equilibrium volume. (In fact this is also a reason why we have chosen an "experimental" reference volume $V_0 = 69.578$ Å^3 which is close to the lower of the two values 69.536 and 69.85 Å^3 given in Ref. 5. The actual value chosen for V_0 is not very critical as long as it is in the range corresponding to the relative experimental errors,[5] 6×10^{-4} on the volumes.) Values of zero-pressure volumes and bulk moduli are given in Table I.

Figures 3–6 show the calculated c/a and u parameters in comparison to the experimental[5] data. In general, the calculated structural parameters agree well with experiments, but whereas the u parameters calculated with the LDA almost match experiments over the full volume range, the GGA results are systematically somewhat too large. Also for c/a LDA seems to yield results which are closer to the experimental values than those obtained with the GGA. In particular the GGA values differ from the measured axial ratios for large volumes (see Table II).

Figure 3 of Ref. 5 shows that the slope of c/a vs P changes markedly at 5 GPa. At this pressure the volume is 64 Å^3, and Fig. 4 also shows this change of slope, approximately by a factor of 2, in the experimental data when plotted against volume. On the other hand, the calculated c/a (GGA) "curve" does not reproduce the observed slope change at 64 Å^3. However, for volumes above ≈ 70 Å^3 the calculated slope is similar to what is found in the experiment. We return to this point in Sec. IV A. A small anomaly, most visible in Fig. 3, is found near $V = 57$ Å^3. Repeated calcula-

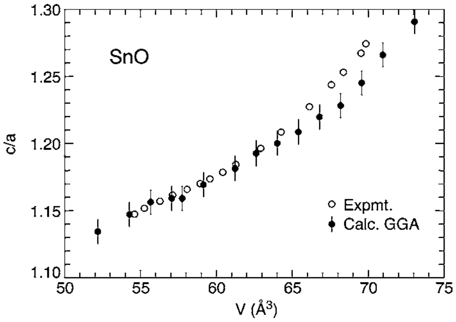

FIG. 4. As Fig. 3, but with calculated values obtained by the GGA.

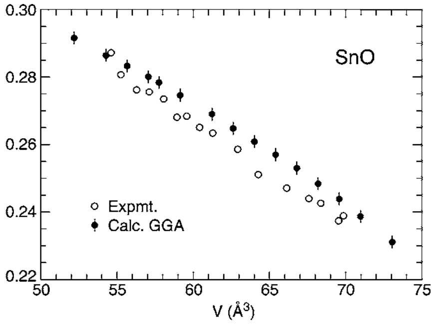

FIG. 6. As Fig. 5, but with calculated values obtained by the GGA.

TABLE II. Structural parameters c/a and u versus relative volume V/V_0, where the (experimental) equilibrium volume $V_0 = 69.578$ Å^3. The columns "expmt." are experimental data from Ref. 5, but after interpolation.

	c/a			u		
V/V_0	Expmt.	LDA	GGA	Expmt.	LDA	GGA
0.80	1.1561	1.166	1.157	0.2814	0.2784	0.2833
0.83	1.1658	1.167	1.159	0.2743	0.2731	0.2784
0.85	1.1738	1.176	1.170	0.2697	0.2695	0.2646
0.88	1.1882	1.185	1.182	0.2630	0.2639	0.2690
0.90	1.1993	1.200	1.193	0.2588	0.2596	0.2648
0.92	1.2116	1.210	1.200	0.2546	0.2553	0.2609
0.94	1.2252		1.209	0.2506		0.2570
0.96	1.2400	1.230	1.220	0.2468	0.2477	0.2530
0.98	1.2560	1.246	1.228	0.2430	0.2429	0.2484
1.00	1.2733	1.255	1.245	0.2394	0.2386	0.2439

tions with a very dense mesh in k space did not remove the small step. The experimental data do not exhibit a similar feature.

The electric field gradient usually depends sensitively on structural details, and therefore we examined whether this quantity in SnO would reflect the change of slope in c/a vs P. The electric field gradient tensor $\overline{\overline{V}}$ is calculated using the nonspherical part (in fact, the $\ell = 2$ component) of the crystalline Hartree potential, from which the second derivative tensor

$$V_{ij} = \frac{\partial^2 V_{H,\ell=2}}{\partial x_i \, \partial x_j}$$

is obtained (evaluated at the nuclear positions). Denoting the eigenvalues of $\overline{\overline{V}}$ by V_{xx}, V_{yy}, and V_{zz} with $|V_{xx}| \leq |V_{yy}| \leq |V_{zz}|$, the electric field gradient per definition is equal to V_{zz}, while the asymmetry parameter is

$$\eta = \frac{V_{xx} - V_{yy}}{V_{zz}},$$

which lies in the range $[0,1]$ (since $V_{xx}+V_{yy}+V_{zz}=0$). Due to the symmetry of the litharge crystal structure, the major axis of the EFG tensor ("z direction") is along the c axis, and the asymmetry parameter η is zero.

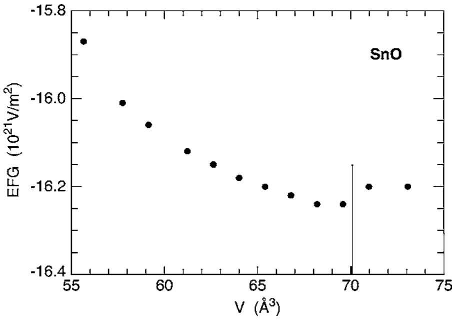

FIG. 7. Calculated electric field gradient (EFG) on the Sn site vs volume (V) obtained by the GGA. The vertical line indicates the volume where the minimal gap closes in this band structure calculation.

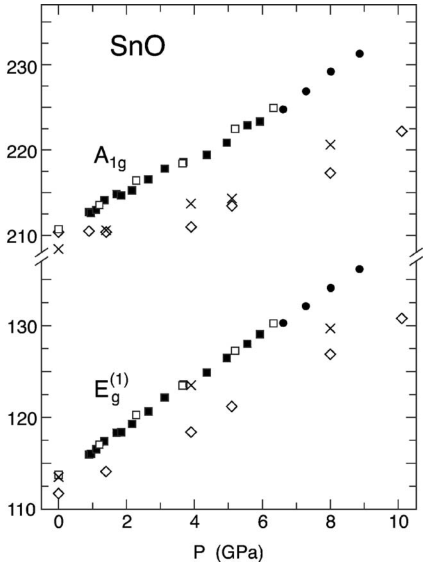

FIG. 8. Frequencies of the tin modes A_{1g} and $E_g^{(1)}$ in SnO vs pressure. The filled squares, open squares, and filled circles are experimental data from Ref. 5. The crosses represent "frozen phonon" calculations within the LDA using the LAPW method, whereas similar calculations obtained by means of the LMTO method are shown as diamonds.

Figure 7 shows the volume variation of the Sn-EFG calculated within the GGA, but using experimental (but interpolated and extrapolated) u and c/a values. Maybe a change of slope starting near $V = 64$ Å^3 can be detected and related to the abovementioned change in the c/a variation, but otherwise the only significant "anomaly" is found near $V = 70$ Å^3. Tentatively, we associate this with the insulator-metal transition since the gap in the GGA band structure closes at the volume indicated by the vertical line, see the next section. The EFGs have been calculated[42] for a series of tin compounds, also SnO. At equilibrium volume, using slightly different structural parameters, the Sn-EFG was found to be -16.37×10^{21} V/m^2. Using the magnitude $|Q| = 12.8 \pm 0.7$ fm^2 of the quadrupole moment of the excited ^{119}Sn nucleus from Ref. 42, our value (at V_0) of the EFG corresponds to a quadrupole splitting of 1.31 ± 0.07 mm/s. This

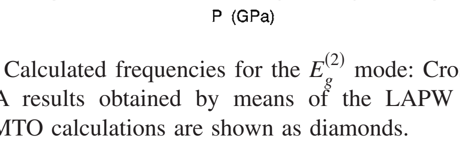

FIG. 9. Calculated frequencies for the $E_g^{(2)}$ mode: Crosses represent LDA results obtained by means of the LAPW method, whereas LMTO calculations are shown as diamonds.

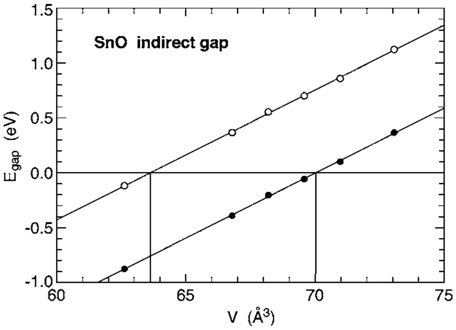

FIG. 10. Calculated volume variation of the minimal (indirect) gap in SnO. Filled circles represent the GGA calculations while the open circles are the same calculations, but upshifted so that the gap is 0.7 eV at the equilibrium volume (V_0=69.578 Å^3). The value 0.7 eV for the experimental gap was mentioned in Ref. 7. With this, the present calculations suggest that the gap is closed for volumes below 63.6 Å^3.

agrees well with experiments, 1.35 mm/s,[43] and 1.335(3) mm/s.[9]

Zone center phonons for SnO at $P=0$ were calculated within the LDA by the FP-LMTO method in Ref. 8 and by means of the FP-LAPW method in Ref. 44. Koval *et al.*[44,45] further used the shell model to investigate the lattice dynamics and calculate the Mössbauer recoilless fraction and specific heat. We have here calculated the Γ modes A_{1g}, the $E_g^{(1)}$ (tin), and the $E_g^{(2)}$ (oxygen) modes as functions of pressure. The calculated frequencies are shown in Figs. 8 and 9. The Sn modes, Fig. 8, are compared to the Raman data obtained in Ref. 5. There are no experimental data available for the $E_g^{(2)}$ mode.

For the $E_g^{(1)}$ mode our calculations agree rather well with experiments considering the frequencies and their pressure variation. The calculated pressure variation of the A_{1g} frequencies differs more significantly from the experiment. In particular we found only a weak increase in the frequency in the pressure range 0 to 4 GPa. For all three modes, Figs. 8 and 9, we found that the LAPW and LMTO calculations agree quite well. Further, we also performed the calculations using the GGA and found only insignificant differences from the LDA results.

The LDA calculation for zero pressure by Koval *et al.*[44] gave for A_{1g} ω=212 cm^{-1} and for $E_g^{(1)}$ the frequency ω =113 cm^{-1}, i.e., almost the same values as here, and also in excellent agreement with the experimental results.[5] The LMTO values obtained in Ref. 8 were 211 and 143 cm^{-1}, for A_{1g} and $E_g^{(1)}$, the latter being too high. A reason for this may be related to difficulties in performing reliable k-space integrations for SnO, even at $P=0$ due to the small or negative band gap in the LDA and GGA band structures. In the present work it was examined whether such problems could cause the pressure coefficients calculated for the A_{1g} frequency to be too low. Therefore we repeated the (FP-LMTO) calculations using the k-space sampling in the "semiconductor" mode (Sec. II), but the results were not affected. Even increasing the k-point density had no effect. Also, the frozen-phonon distortions, minimum 16, were all sufficiently small to exclude errors due to anharmonicity. Effects caused by insufficient convergence in basis set size were excluded as well. Since we also compared two quite different methods FP-LMTO and FP-LAPW and applied both GGA and LDA (in both schemes), we conclude that the computational accuracy of phonon frequencies which we can reach for SnO with our methods is ≈5%, or our model does not include all interactions which influence the phonons in the real system, the experiment.

IV. BAND STRUCTURES AND HYBRIDIZATION

Several publications have discussed the bonding in SnO and PbO, as mentioned in the Introduction. The latest detailed study by Raulot *et al.*[10] drew conclusions which are similar to what we find, and they also applied similar methods. Therefore, this section will contain just a few remarks on this matter. The pressure-induced insulator-metal transition is of particular interest, and although the LDA and GGA calculations yield too low gap values, and the experimental

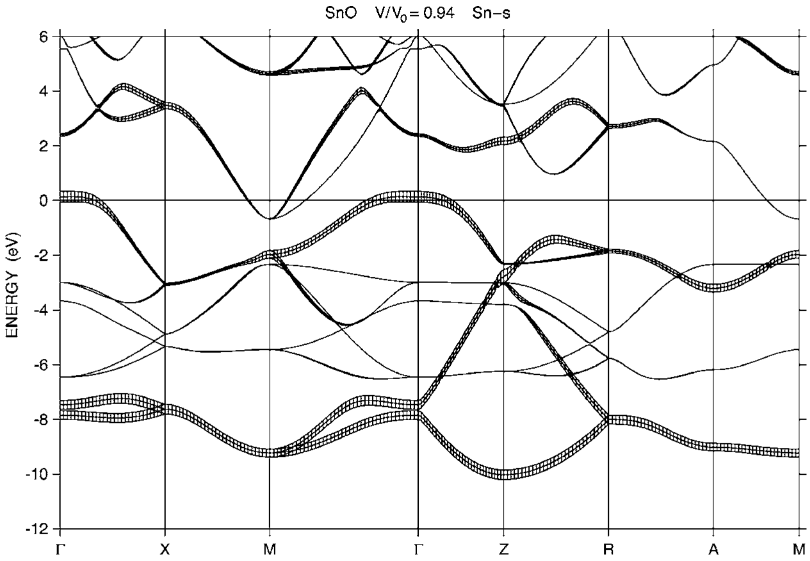

FIG. 11. Band structure of SnO, TB-LMTO-ASA, LDA, at V/V_0=0.94. Structural parameters c/a=1.2252 and u=0.2506 (Table II). The "fat bands" illustrate the Sn-s content in the conduction bands and O-2p bands. Energies are relative to the Fermi level.

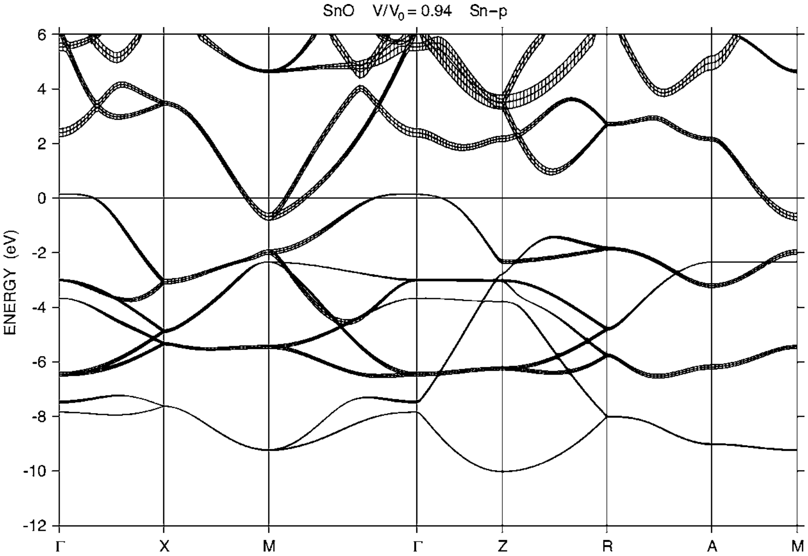

FIG. 12. As Fig. 11, but the "fat" bands here illustrate the Sn-p content.

zero-pressure minimal gap may be ill defined, we shall nevertheless argue that gap closure should occur around 5 GPa. Section IV A concerns SnO, and in Sec. IV B we compare the role of lone pairs in SnO and PbO.

A. SnO

The band structure calculations made for SnO at the equilibrium volume have a fundamental gap which is zero, or slightly negative, see below. Due to the usual "LDA gap problem" LDA as well as GGA calculations yield too small gap values. At equilibrium the correct minimum gap is around 0.7 eV.[7]

We can infer, however, from the calculations that the gap is indirect, the conduction band minimum being at the M point and the valence-band maximum at Γ. The FP-LMTO (GGA) calculations gave for the relative volumes $V/V_0 = 1.05$, 1.02, 1.00, 0.98, 0.96, and 0.90 the gap values 366, 101, $-57, -203, -391$, and -857 meV, respectively, and these results are marked with filled circles in Fig. 10. If we assume that the gap error in the calculation is similar at all volumes, we obtain an estimate of the gaps E_{gap} in "real SnO" simply by adding 757 meV to the GGA values, 0.7 eV (experimental gap) minus the theoretical gap (-57 meV) at $P=0$. The open circles in Fig. 10 show the estimated E_{gap} vs volume, and the closing[46] of the gap obtained in this way occurs at $V=63.6$ Å^3 From Fig. 2 it is seen that the experimental pressure at this volume is ≈4.8 GPa and the theoretical (GGA) around 6.1 GPa. This is in excellent agreement with the experimental estimate[5] of the gap closure pressure ≈5 GPa.

We calculated, for $V/V_0=0.94, dE_{\mathrm{gap}}/d\ln(c/a)$ to be 20.7 eV, i.e., the gap depends very sensitively on the interlayer distance. An increase, at this volume, of c/a from 1.2252 to 1.2735 would be required to produce a (slightly) positive gap in the LDA band structure. Such an increase, however, exceeds both the experimental and the theoretical uncertainties in the axial ratios as well as the difference between the calculated and measured values.

It was earlier, Sec. III, mentioned that the slope of c/a vs V measured in Ref. 5 changes as the volume is reduced below 64 Å^3, and that Fig. 4 exhibits a similar change, however, at a larger volume ≈70 Å^3. Considering then experiment as well as theory it appears that the change in slope of c/a and the closure of the gap occur at the same volume, or pressure, which in "real SnO" is ≈5 GPa, but ≈0 in "GGA SnO." It should be mentioned the we did similar calculations within the LDA and found very similar results.

The Figs. 11 and 12 show the SnO band structure (TB-LMTO-ASA). A volume $V/V_0=0.94$ was chosen, in fact the zero-pressure volume calculated within the LDA. At this compression "real SnO" would still have a positive minimum gap. The occupied bands are mainly of O-p character, but we have here chosen to illustrate, by means of "fat bands,"[36,47] the content of Sn-s and Sn-p character. As shown in the same way in Ref. 10 there is a strong hybridization between the O-p and the Sn-s states (Fig. 11). This shows

FIG. 13. (Color online) Electron localization function calculated, in a (100) plane, for PbO (equilibrium volume) in a non relativistic approach. Low-valued contours are dark blue, the highest magenta. The highest value is 0.946, and the step in contour values is 0.035.

FIG. 14. (Color online) Electron localization function calculated, with inclusion of relativistic effects, for PbO (equilibrium volume) same contour values as in Fig. 13.

that the intralayer contribution from the lone pair to the bonding is important. The second figure, Fig. 12 shows that the occupied bands have only small Sn-*p* components, and above the Fermi level where the states have a pronounced Sn-*p* character, the Sn-*s* content is low. Again, the Sn-*s* lone pair interacts with O-*p*, not Sn-*p* as a "classical" picture would suggest (and which indeed is the case in sp^3 bonded pure α-tin).

B. Comparison between the role of the lone pairs in SnO and PbO

Our calculated electron localization functions for SnO are very similar to those presented by Raulot *et al.*[10] (same method, same code). We also agree with Ref. 10 in the statement that the lone pair in SnO plays a more significant role in the bonding than the lone pair (Pb-6*s*) in PbO due to the relativistic mass-velocity downshift being larger in the heavy element Pb than in Sn. Raulot *et al.* illustrate this by comparing the ELFs of SnO and PbO and observe that there is less localization in SnO than in PbO. This reflects[10] that SnO is "the better metal," PbO being an insulator with a significant gap and SnO a semimetal at ambient conditions. We shall here examine the influence of the relativistic effects in PbO more directly, namely by comparing relativistic and non-relativistic calculations for PbO. The latter are simply performed by setting the speed of light to infinity in the Dirac equation for the radial waves of the MTOs.

The Figs. 13 and 14 show the ELF as calculated for PbO without (Fig. 13) and with inclusion of relativistic effects. (We use the "experimental" structural parameters from Table 1 in Ref. 10.) It is seen that there is more tendency to localization in the case where relativity is taken into account than for the "nonrelativistic PbO," compare, for example, the regions below the Pb atoms. Also, the dark-blue areas, low ELF values, are larger in the relativistic than in the nonrelativistic case. The ELF of "nonrelativistic PbO" is more similar to SnO than to "real PbO." This becomes even clearer if we compare the band structures. The calculated bands of "nonrelativistic PbO" are shown in Fig. 15. Clearly, this band structure resembles very much that of SnO. There is a small overlap between valence and conduction bands due to the "LDA gap problem," and further the hybridization between the metal-*s* and oxygen-*p* states is also very similar to what was found for SnO. If we, on the other hand, include the relativistic effects it is seen, Fig. 16, that the PbO band structure, even in the LDA, exhibits a significant indirect gap, and simultaneously the down shift of the 6*s* states reduces considerably the hybridization between the lone pair and the upper and central parts of the valence band complex. This is an example of what Phillips[48] called relativistic dehybridization effects. Other examples may be found in Refs. 49–51.

This effect is also found in pure Pb,[50] where this downshift implies that the magnitude (cost) of the $s \rightarrow p$ promotion energy exceeds the energy gained by formation of sp^3 bonding hybrids. Therefore Pb cannot form in the diamond structure, the one found for the other group-IV elements. Also, in Ref. 50 it was shown that "nonrelativistic Pb" is quite similar to Sn, even with respect to bond order.

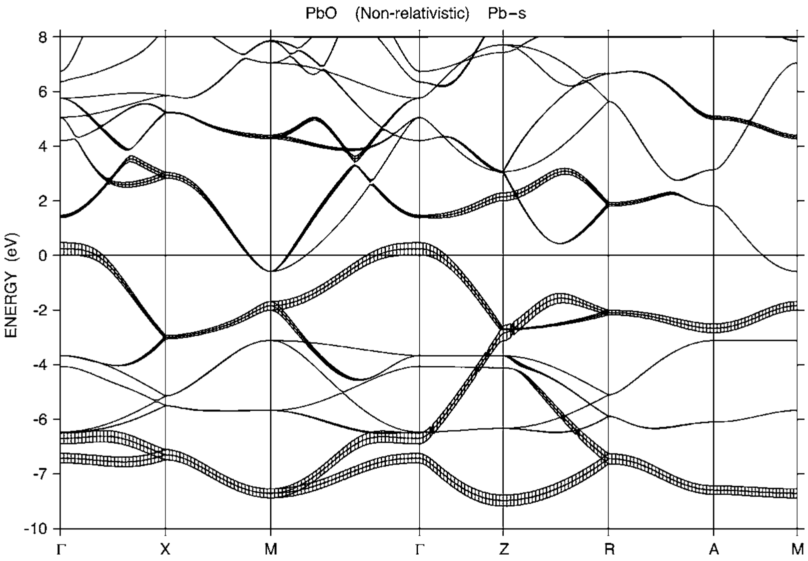

FIG. 15. Band structure with Pb-*s* fat bands calculated for PbO in a nonrelativistic approach. Compare to (relativistic) SnO, Fig. 11. Energy zero corresponds to the Fermi level.

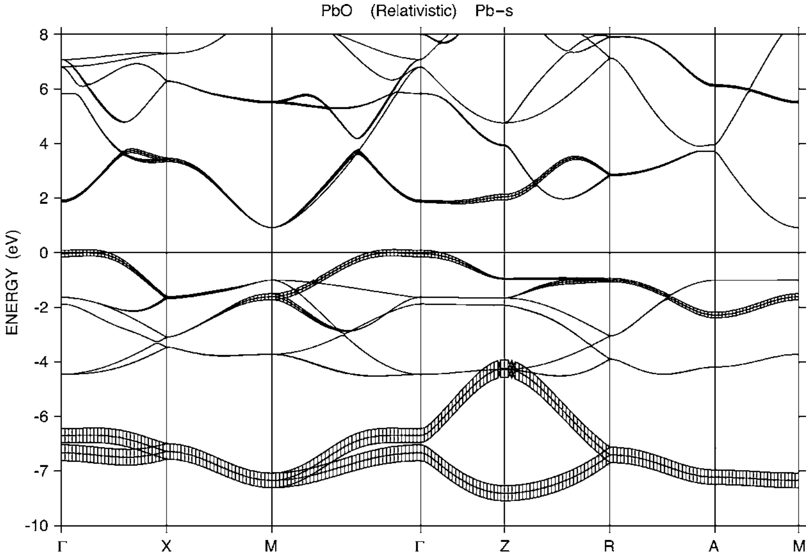

FIG. 16. Band structure with Pb-*s* fat bands calculated for PbO in a relativistic approach (spinorbit splitting omitted). Zero energy at the valence-band maximum.

V. CONCLUSIONS

The present *ab initio* calculations of the electronic structure of SnO confirm the picture of the role of the Sn lone pair in the bonding in this compound given recently by Raulot *et al.*[10] and others. The lone pair is not inert, it hybridizes with the oxygen *p*-states, *not* (much) with Sn-*p*. The interaction is mainly intralayer. A comparison between relativistic and nonrelativistic calculations for PbO showed that the bands, electron localization functions, and the metal-*s* oxygen-*p* hybridization are very similar in SnO (relativistic calculation) and "nonrelativistic" PbO. Inclusion of relativistic shifts in the PbO calculation reduces the hybridization, the so-called relativistic dehybridization effect.

Although the LDA and GGA lead to too small band gap values in semiconductors, we estimated that applying pressure to SnO causes the indirect minimal gap to close around 5 GPa. The gap depends sensitively on the distance between the layers in the litharge structure $dE_{\mathrm{gap}}/d\ln(c/a) \approx 21$ eV.

The calculated structural parameters agree very well with recent high-pressure experiments,[5] in particular, for P above 5 GPa. In this regime both the "real SnO" and the "theoretical SnO" (with underestimated gap) are metallic. This, and the fact that we for volumes where the GGA gap has opened find the same pressure coefficient for c/a as observed, indicate a relation between the kink observed[5] at 5 GPa and the insulator-metal transition. Tentatively, it is suggested that the insulator-metal transition could be observed in the behavior of the electric field gradient (quadrupole splitting) as the external pressure is varied.

The theoretical A_{1g} and E_g phonon frequencies agree within $\approx 5\%$ with experiments,[5] but for A_{1g} we find a pressure coefficient which is too small in the range 0 to 4 GPa. In spite of a careful search for possible numerical inaccuracies we were not able to explain this discrepancy. It should be mentioned, however, that during the frozen-phonon calculations we observed that the A_{1g} mode couples strongly to the electron system, especially the states at the edges of the minimum gap. Possible consequences of this will be the subject of further investigations.

ACKNOWLEDGMENTS

The authors would like to thank K. Syassen for fruitful discussions and for having made the work of Ref. 5 available to us prior to publication as well as for giving us permission to include Fig. 1. The numerical calculations were performed at the Centre for Scientific Computing in Aarhus, mainly financed via the *Danish Centre for Scientific Computing*, DCSC. Further, funding from the Danish Natural Science Research Council, Grant No. 21-03-0340, is gratefully acknowledged.

---

[1] R. W. G. Wyckoff, *Crystal Structures* (Wiley, New York, 1965), Vol. 1.

[2] N. R. Serebryaya, S. S. Kabalkina, and L. F. Vereshchagin, Dokl. Akad. Nauk SSSR **187**, 307 (1969).

[3] D. M. Adams, A. G. Christy, J. Haines, and S. M. Clark, Phys. Rev. B **46**, 11 358 (1992).

[4] K. Suito, N. Kawai, and Y. Masuda, Mater. Res. Bull. **10**, 677, (1975).

[5] X. Wang, F. X. Zhang, I. Loa, K. Syassen, M. Hanfland, and Y.-L. Mathis, Phys. Status Solidi B **241**, 3168 (2004).

[6] J. Geurts, S. Rau, W. Richter, and F. J. Schmitte, Thin Solid Films **121**, 217 (1984).

[7] K. M. Krishna, M. Sharon, M. i K. Mishra, and V. R. Marathe, Electrochim. Acta **41**, 1999 (1996).

[8] E. L. Peltzer y Blancá, A. Svane, N. E. Christensen, C. O. Rodriguez, C. O. Cappannini, and M. S. Moreno, Phys. Rev. B **48**, 15 712 (1993).

[9] I. Lefebvre, M. A. Szymanski, J. Olivier-Fourcade, and J. C. Jumas, Phys. Rev. B **58**, 1896 (1998).

[10] J.-M. Raulot, G. Baldinozzi, R. Sashadri, and P. Cortona, Solid

State Sci. **4**, 467 (2002).

[11] M. Meyer, G. Onida, M. Palummo, and L. Reining, Phys. Rev. B **64**, 045119 (2001).

[12] G. Trinquier and R. Hoffmann, J. Phys. Chem. **88**, 6696 (1984).

[13] H. J. Terpstra, R. A. de Groot, and C. Haas, Phys. Rev. B **52**, 11 690 (1995).

[14] G. W. Watson, S. C. Parker, and G. Kresse, Phys. Rev. B **59**, 8481 (1999).

[15] W. Kohn and L. J. Sham, Phys. Rev. **140**, A1133 (1965).

[16] D. M. Ceperley and B. J. Alder, Phys. Rev. Lett. **45**, 566 (1980).

[17] J. P. Perdew and A. Zunger, Phys. Rev. B **23**, 5048 (1981).

[18] J. P. Perdew, K. Burke, and M. Ernzerhof, Phys. Rev. Lett. **77**, 3865 (1996).

[19] J. P. Perdew and Y. Wang, Phys. Rev. B **45**, 13 244 (1992); J. P. Perdew, J. A. Chevary, S. H. Vosko, K. A. Jackson, M. R. Pederson, D. J. Singh, and C. Fiolhais, Phys. Rev. B **46**, 6671 (1992).

[20] Y. Zhang and W. Yang, Phys. Rev. Lett. **80**, 890 (1998).

[21] J. P. Perdew, K. Burke, and M. Ernzerhof, Phys. Rev. Lett. **80**, 891 (1998).

[22] S. Tinte, M. G. Stachiotti, C. O. Rodriguez, D. L. Novikov, and N. E. Christensen, Phys. Rev. B **58**, 11 959 (1998).

[23] E. L. Peltzer y Blancá, C. O. Rodriguez, J. Shitu, and D. L. Novikov, J. Phys.: Condens. Matter **13**, 9463 (2001).

[24] N. E. Christensen, in *High Pressure in Semiconductor Physics I*, edited by T. Suski and W. Paul, Vol. 54 of Semiconductors and Semimetals (Academic, New York, 1998), p. 49.

[25] K. Takemura, N. E. Christensen, D. L. Novikov, K. Syassen, U. Schwarz, and M. Hanfland, Phys. Rev. B **61**, 14 399 (2000).

[26] N. E. Christensen and D. L. Novikov, Solid State Commun. **119**, 477 (2001).

[27] O. K. Andersen, Phys. Rev. B **12**, 3060 (1975).

[28] M. Methfessel, Phys. Rev. B **38**, 1537 (1988).

[29] M. Methfessel, C. O. Rodriguez, and O. K. Andersen, Phys. Rev. B **40**, 2009 (1989).

[30] M. van Schilfgaarde (private communication).

[31] D. L. Novikov (private communication) and Ref. 26, and references therein.

[32] D. Singh, Phys. Rev. B **43**, 6388 (1991).

[33] P. Blaha, K. Schwarz, G. K. H. Madsen, D. Kvasnicka, and J. Luitz, WIEN2K, Vienna, 2001, http://www.wien2k.at

[34] A. D. Becke and K. E. Edgecombe, J. Chem. Phys. **92**, 53 (1990).

[35] B. Silvi and A. Savin, Nature (London) **371**, 683 (1994).

[36] R. W. Tank, O. Jepsen, A. Burkhardt, and O. K. Andersen, The Stuttgart TB-LMTO-ASA program (lmto46), Max-Planck Institut für Festkörperforschung, Stuttgart, Germany, 1996.

[37] O. Jepsen and O. K. Andersen, Solid State Commun. **9**, 1763 (1971).

[38] G. Lehmann and M. Taut, Phys. Status Solidi B, **54**, 469 (1972).

[39] P. E. Blöchl, O. Jepsen, and O. K. Andersen, Phys. Rev. B **49**, 16 223 (1994).

[40] M. Fanciulli, C. Rosenblad, G. Weyer, A. Svane, N. E. Christensen, and H. von Kanel Phys. Rev. Lett. **75**, 1642 (1995).

[41] M. Fanciulli, A. Zenkevich, I. Wenneker, A. Svane, N. E. Christensen, and G. Weyer, Phys. Rev. B **54**, 15 985 (1996).

[42] A. Svane, N. E. Christensen, C. O. Rodriguez, and M. Methfessel, Phys. Rev. B **55**, 12 572 (1997).

[43] R. H. Herber, Phys. Rev. B **27**, 4013 (1983).

[44] S. Koval, R. Burriel, M. G. Stachiotti, M. Castro, R. L. Migoni, M. S. Moreno, A. Varela, and C. O. Rodriguez, Phys. Rev. B **60**, 14 496 (1999).

[45] S. Koval, M. G. Stachiotti, R. L. Migoni, M. S. Moreno, R. C. Mercader, and E. L. Peltzer y Blancá, Phys. Rev. B **54**, 7151 (1996).

[46] The minimal (indirect) gap depends sensitively on c/a, as mentioned in the text. Therefore it is important that the gaps displayed in Fig. 10 are calculated with the optimized structural parameters at each volume. The gaps were calculated for volumes above as well as below the theoretical LDA/GGA insulator-metal transition. The almost linear variation of the gap with volume suggests that the gap deformation potential is constant for volumes in the range ≈ 62 to 73 Å^3. The gap values used here were obtained within the GGA, but LDA calculations yield similar values. Furthermore, it is the experience from numerous calculations for semiconductors, that gap deformation potentials are well reproduced by LDA/GGA calculations even in cases where these approximations seriously underestimate the gap itself.

[47] M. Alouani (private communication).

[48] J. C. Phillips, *Bonds and Bands in Semiconductors* (Academic, New York, 1973).

[49] N. E. Christensen and J. Kollár, Solid State Commun. **46**, 717 (1983).

[50] N. E. Christensen, S. Satpathy, and Z. Pawlowska, Phys. Rev. B **34**, 5977 (1986).

[51] N. E. Christensen, in *Relativistic Electronic Structure Theory*, Vol. 11 of Theoretical and Computational Chemistry, edited by P. Schwerdtfeger (Elsevier, Amsterdam, 2002), Pt. 1, p. 863.